

Effect of different preparation conditions on the properties of nano-hydroxyapatite/bamboo fiber composite membrane

Jiang Liuyun (✉ jlytxg@163.com)

College of Chemistry and Chemical Engineering, Hunan Normal University <https://orcid.org/0000-0002-8592-5736>

Zhihong Jiang

Hunan Normal University

Bingli Ma

Hunan Normal University

Yingjun Ma

Hunan Normal University

Yue Wen

Hunan Normal University

Na Zhang

Hunan Normal University

Yan Zhang

Hunan Normal University

Shengpei Su

Hunan Normal University

Xiongui Tang

Hunan Normal University

Xiang Hu

Hunan Normal University

Research Article

Keywords: Bamboo fiber, nano-hydroxyapatite, composite membrane, degradation

Posted Date: April 25th, 2022

DOI: <https://doi.org/10.21203/rs.3.rs-1503964/v1>

License:   This work is licensed under a Creative Commons Attribution 4.0 International License.

[Read Full License](#)

Effect of different preparation conditions on the properties of nano-hydroxyapatite/bamboo fiber composite membrane

Liuyun Jiang^{* a, b}, Zhihong Jiang^{a, b}, Bingli Ma^{a, b}, Yingjun Ma^{a, b}, Yue Wen^{a, b}, Na Zhang^{a, b}, Yan Zhang^{a, b}, Shengpei Su^{a, b}, Xiongguai Tang^{*c}, Xiang Hu^{*d}

^a National & Local Joint Engineering Laboratory for New Petro-chemical Materials and Fine Utilization of Resources, College of Chemistry and Chemical Engineering, Hunan Normal University, Changsha 410081, PR China

^b Key Laboratory of Chemical Biology & Traditional Chinese Medicine Research (Ministry of Education, China), College of Chemistry and Chemical Engineering, Hunan Normal University, Changsha 410081, PR China

^c College of Physical & Electronic Science, Hunan Normal University, Changsha 410081, PR China

^d State Key Laboratory Developmental Biology of Freshwater Fish, School Life Science, Hunan Normal University, Changsha, 410081, PR China

Abstract

A novel nano-hydroxyapatite/bamboo fiber (n-HA/BF) composite membrane was obtained by a simple casting technique. The membrane forming mechanism and the effects of different forming membrane methods, drying methods and n-HA amounts on the properties of n-HA/BF composite membrane were investigated by Fourier Transform infrared spectroscopy (FT-IR), X-ray diffraction (XRD), scanning electron microscopy (SEM), contact angle, electromechanical universal tester, *in vitro* soaking in simulated body fluid (SBF) and *in vitro* cell culture experiment. The results demonstrated that the dispersity of n-HA nanoparticles in BF matrix was not affected by the preparation condition, however, the morphologies of membrane were determined by the different preparation conditions owing to different hydrogen bond shrinkage. Moreover, the hydrophilicity of the composite membrane was improved under the condition of the membrane formation in oven, freeze drying and high addition content of n-HA, and the mechanical properties of composite membrane depended on n-HA content. *In vitro* soaking behavior indicated that the degradability and bone-like apatite deposition could be controlled by different preparation conditions. And the cell proliferation experiment showed that the n-HA/BF composite membranes obtained under different preparation conditions were all non-toxic. The above results indicated that the casting technique could be used to prepare n-HA/BF composite membrane, and the properties of the composite membrane could be controlled by adopting different preparation conditions, which would have a great promising as guide bone tissue regeneration (GBR) membrane, and the study would provide a new application for BF in biomedical field.

Keywords: Bamboo fiber; nano-hydroxyapatite; composite membrane; degradation

Introduction

Guided bone regeneration (GBR) membrane is commonly used in bone defect, which was placed

Tel.: +86 0731 8887 3111; fax: +86 0731 8887 3111,

E-mail address: jlytxg@163.com, tangxg@hunnu.edu.cn, huxiangsky123123@163.com

43 on the bone defect area as barrier membrane to create a singular space, so as to prevent epithelial
44 cells from growing into the defect, and **permit osteoblasts to proliferate and new bone to form**
45 (Jiang et al., 2015; Niu et al., 2021; Li et al., 2020; 2015). Ideally, GBR membrane should
46 possess appropriate mechanical properties, space-retention ability, biocompatibility and
47 biodegradability (Lee et al., 2016; Yu et al., 2020; Hoornaert et al., 2016). To obtain a satisfactory
48 GBR membrane, natural biodegradable polymers **have** become a research hotspot owing to
49 **better** biocompatibility and biodegradability, compared with the synthetic polymers (Prajatelistia
50 et al., 2021; Ma et al., 2019; Mora-Boza et al., 2020; Bierhalz and Moraes, 2017; Pappu et al.,
51 2019; Gurunathan et al., 2015; Weng et al., 2020).

52 Bamboo fiber (BF) is a natural fiber extracted from bamboo, which has high strength,
53 biodegradability and low cost. Therefore, BF is usually used as a reinforcing agent for polymers
54 (Khalil et al., 2012; Liu et al., 2012; Phuong et al., 2019; Long et al., 2019; Zuo et al. 2019). In
55 our **group**, we have systematically studied and concluded that BF had remarkable reinforce effect
56 on the n-HA/poly (lactide-co-glycolide) (n-HA/PLGA) composite (Li et al., 2015; Jiang et al.,
57 2017; 2018; 2019). Moreover, BF has been used to reinforce **electrospun membrane**
58 (Chingakham et al., 2020; Cai et al., 2018). **However, as we know, casting membrane has denser**
59 **structure**, which would display better mechanical strength and slower degradation than
60 electrospinning membrane (Oksana et al., 2020). **Moreover, casting membrane could be**
61 **prepared by a simple casting technology method**. Therefore, we studied the reinforce effect of
62 carboxylated BF on chitosan-based casting membrane via ionic crosslinking (Tang et al., 2020).
63 However, the preparation procession of carboxylated BF was too tedious. In addition, in the
64 **above-mentioned** study, BF was usually added in the primeval state fiber form as reinforcement,

65 which would be adverse for dispersion, so it would be expected to explore a novel BF-based
66 polymer membrane by a simple and green processing.

67 BF could be dictrectly dissolved into homogeneous solution and casting membrane would be
68 formed, whileas, pure BF membrane lacks osteoconductivity, which would be detrimental to
69 guide bone tissue regeneration, while nano-hydroxyapatite (n-HA) has good osteogenic activity
70 becausee of its similarity with inorganic component of natural bone, so it was normally added
71 into polymeric matrix as nanofiller to endow polymers with better biological performance (Zhao
72 et al., 2018; Muhammad et al., 2017). In addition, in our previous study, we found BF could
73 replace other polymers to develop n-HA/BF nanocomposite by co-precipitation method, and it
74 had a promising to be used as bone materials (Ma et al., 2020). However, whether BF could be
75 replayed other polymers to obtain n-HA/BF composite membrane by solution blending method,
76 and what effects would different preparation conditions produce on the properties of the n-HA/BF
77 membrane, including different forming membrane methods, drying methods and n-HA amounts,
78 and whether the n-HA/BF membrane would be used as GBR membrane, which were all not be
79 reported and it was worth exploring.

80 Based on these, in this work, we attempt to study the fabrication of the n-HA/BF composite
81 membrane by casting method, and the effects of different preparation conditions including
82 forming film methods (in air and in oven), different drying methods (in air, in oven, in freeze
83 dryer) and different n-HA content (10%, 20%, 30% and 40%) on the properties of the n-HA/BF
84 composite membranes were studied by Fourier Transform infrared spectroscopy (FT-IR), X-ray
85 diffraction (XRD), scanning electron microscopy (SEM), contact angle, electromechanical
86 universal teste. Moreover, the degradation behavior of the n-HA/BF composite membrane was

investigated by soaking in simulated body fluid (SBF). Finally, the cell culture experiment was carried out. The main purpose of the work is to demonstrate the feasibility of the fabrication of the n-HA/BF composite membrane by a simple casting method, so as to provide a new GBR membrane by making full use of natural biomass resources.

Experiment Section

Materials

Bamboo fiber (BF) was provided by Zhejiang A&F University, whose size was Φ (0.03-0.2) mm \times (6-10) cm. Dimethylacetamide (DMAc, AR) and LiCl (AR) were purchased from Aladdin. $\text{Ca}(\text{NO}_3)_2 \cdot 4\text{H}_2\text{O}$ (AR), $\text{Na}_3\text{PO}_4 \cdot 12\text{H}_2\text{O}$ (AR), P_2O_5 , and NaOH (AR) were all from Tianjin Fengchuan Chemical Reagent Technologies Co. Ltd.. Other agents were analytical grade.

Preparation of the n-HA/BF composite membranes

Bamboo fiber was dissolved in DMAc/LiCl system with the concentration of 1.3 wt%. A certain amount of n-HA was dispersed in DMAc by ultrasonic treatment, which was slowly added into bamboo fiber solution with the magnetic stirring, and the evenly dispersed mixture solution was poured on the clean and dry glass plate, and the thickness of the membrane was adjusted by the glass rod with two copper rings. Then, the glass plate covered with n-HA/BF mixture solution was put in air or in oven (70 °C) to form film, afterword, it was dried in air, in oven (70 °C) or freeze drying, thus, n-HA/BF composite membrane with 20% n-HA were obtained by six methods, and the membranes were noted as air-air, air-oven, air-freeze drying, oven-air, oven-oven and oven-freeze drying, respectively. Moreover, n-HA/BF composite membrane with different n-HA contents of 10 %, 20 %, 30 % and 40 % n-HA were prepared by air-air method in the similar procedure.

109 Characterization of the composite membranes

110 The appearance of the membranes acquired by the two different preparation methods of air-oven
111 and oven-oven were given as examples, which was taken by normal digital camera.

112 Thermo Nicolet 670 spectrometer was used to analysis the Fourier transformation infrared
113 (FTIR) of samples, and the collected spectrum range was 600~ 4000 cm^{-1} .

114 The phase analyses of samples were carried out by X-ray diffraction (XRD) (a Rigaku
115 Corporation X-ray diffractometer) with Cu-K α radiation, the scanning speed of 5°/min at 40 kV
116 and 45 mA, the range of $2\theta=10\sim70^\circ$.

117 The morphologies of samples treated with the gold sputtering were observed by scanning
118 electron microscopic (SEM, S-520, Hitachi, Japan).

119 The contact angles of samples were measured with rotating drop interfacial tensiometer
120 (TX500TM, Kono, USA). The sample was put on the slide, and the distilled water was dropped
121 onto the membrane surface by stop drop method, then the water drop on the sample was
122 observed.

123 The tensile strengths of samples with the size of 0.2 mm \times 4 mm \times 60 mm were measured by
124 electromechanical universal testing machine (WDW-20, China) with the speed of 5 mm/min
125 under 60 % relative humidity at room temperature, and the mean value was calculated based on
126 the five parallel samples of each specimen.

127 *In vitro* degradation of the composite membranes

128 The degradation of n-HA/BF composite membrane *in vitro* was studied by soaking in SBF,
129 whose ion concentration was very similar to that of human plasma, and it was obtained according
130 to the following procedure, that is, NaHCO_3 (0.350 g), NaCl (7.996 g), KCl (0.224 g), K_2HPO_4 ·

131 3H₂O (0.228 g), CaCl₂ (0.278 g), Na₂SO₄ (0.071 g), MgCl₂ · 6H₂O (0.305 g) were dissolved in
132 deionized water in order, and buffer with trimethylolmethyaminomethane (6.057 g) and
133 hydrochloric acid to adjust the solution to physiological pH=7.40 at 37 °C (± 0.5°C). The samples
134 were taken out from SBF at 2, 4, 6 and 8 weeks, and filter paper was used to absorb surface
135 residual washing water. The weight loss rate and water absorption were calculated as follows.

136
$$\text{Weight loss rate } \%/=(w_1-w_3)/w_1 \times 100\%$$

137
138
$$\text{Water absorption } \%/=(w_2-w_3)/w_3 \times 100\%$$

139
140 The original weight of the sample was noted as W₁, and the wet weight and the dry weight
141 was noted as W₂ and W₃, respectively, after being entirely dried after soaking.

142 *In vitro* cell biocompatibility of the composite membranes

143 Bone mesenchymal stem cells (BMSCs) were used to primarily assess *in vitro* cells viability,
144 which was isolated according to the related literature (Hoseini et al., 2015; Ye et al., 2019). The
145 samples with the thickness of 0.2 mm and diameter of 6.0 mm were cleaned with 75 % ethanol
146 solution, sterilized under ultraviolet lamp. The treated samples were placed in a 96-well plate
147 with the density of 4000 cells/well without disturbed in an incubator for 3 hours, then an
148 additional 1 mL culture medium was added into each well.

149 The cell proliferation was evaluated by MTT (3-(4,5-dimethylthiazol-2-yl)-2,5-diphenyl-2H-
150 tetrazolium bromide) assay (Priyadarshini et al., 2018; Shakeri et al., 2014; Hivechi et al., 2021).

151 At designated time of 1, 2 and 3 days, the medium for the cell-seeded materials were discarded,
152 and 100 µL MTT solution with 3 mg/mL was added, incubated at 37 °C in an air atmosphere
153 containing 5 % CO₂ for at least 4 hours, and 100 µL DMSO was added to dissolve the formazan
154 crystals. Then the 200 µL purple solution was absorbed and transferred into a new 96-well plate,

and the optical density (OD) values of the solution were measured in microplate reader (Synergy HTX, BIOTEK, USA) at 495 nm.

Results and discussion

Characterization of surface-modified n-HA

Appearance of the membranes

Fig. 1 displays the n-HA/BF composite membrane appearance, it can be seen that the membrane formed in air had smaller area and thicker than that formed in oven, which was mainly caused from the different changes of the hydrogen bonds between the bamboo fiber molecules. In air, the bamboo fiber was easy to absorb the water, which would make the hydrogen bond shrinkage in the bamboo fiber, thus the bamboo fiber was gelled and DMAC/LiCl solution precipitated from the edge, resulting in thicker film and smaller area. While in oven, DMAC solvent was easy to volatilize and the hydrogen bond between the bamboo fiber molecules was destroyed, and the bamboo fiber has been formed before shrinkage, resulting in thinner film and larger area.

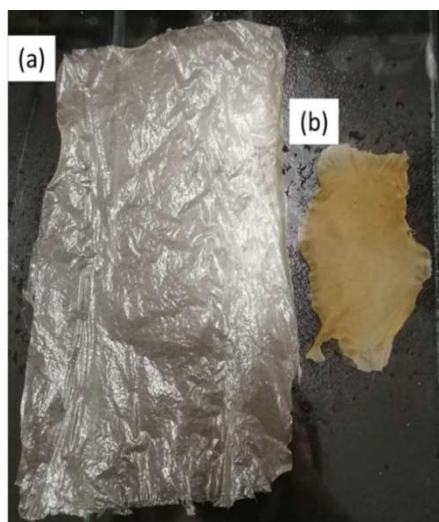


Fig.1. Membrane appearances formed by different conditions. (a) in oven, (b) in air.

IR analysis

Fig. 2 is the FT-IR spectra of different n-HA/BF composite membrane obtained by different

methods and different n-HA contents. The characteristic peaks of 2920 cm^{-1} and 2846 cm^{-1} corresponded to the tensile vibration of C-H bond on methylene of BF existed in n-HA/BF composite membrane. In addition, the characteristics peaks at 3567.2 cm^{-1} attributed to the tensile vibration of OH^- and the peaks at 1095 cm^{-1} , 604 cm^{-1} and 565 cm^{-1} of PO_4^{3-} were related to n-HA (Chesley et al., 2020). The peak position did not transfer obviously when n-HA was added into BF, which indicated that n-HA was simply blended with BF without chemical change. Compared with the membrane formed in oven and in air, the peak intensity of the film formed in oven was markedly weakened, for example, the sharp peak at 1043 cm^{-1} , which was caused by less substance in the unit area for the thinner film formed in oven. Additionally, for the different n-HA/BF composite membrane with different n-HA contents, there was no obvious difference for the characteristics peak.

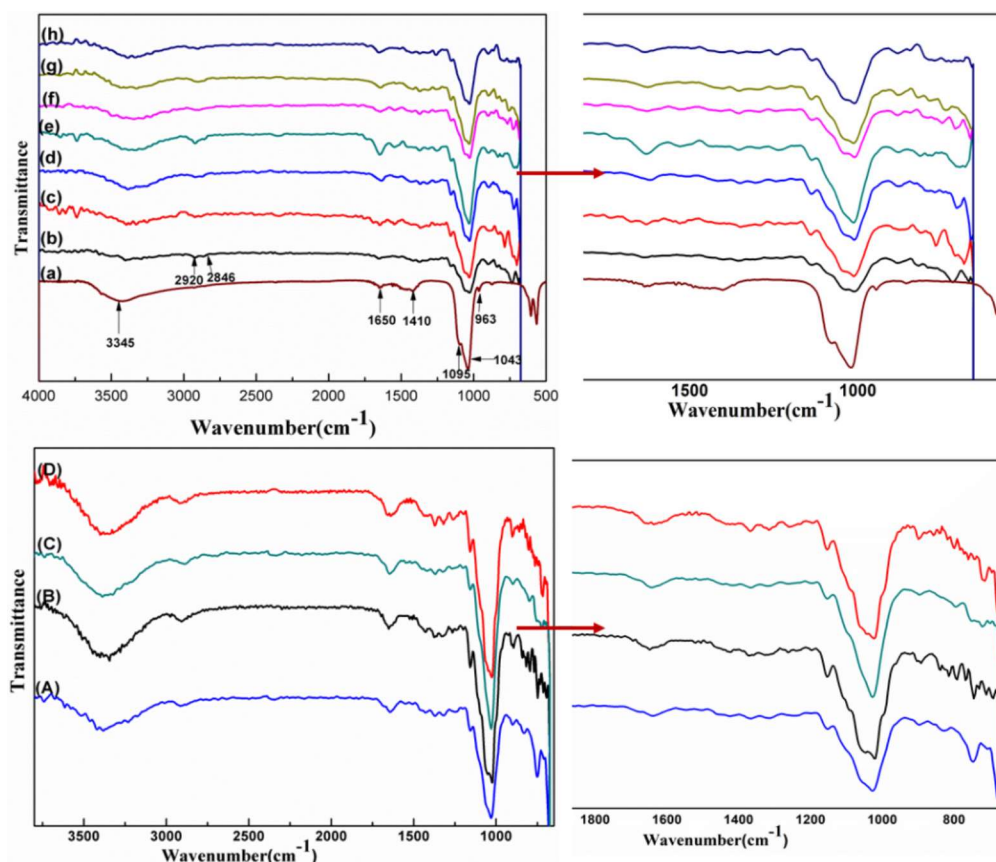


Fig.2. FTIR spectra of samples. (a)n-HA, (b)BF, (c)Air-Air, (d)Air-oven, (e)Air-freeze drying, (f) Oven-air, (g)Oven-oven, (h)Oven-freeze drying, (A)10% n-HA/BF, (B)20% n-HA/BF, (C) 30% n-HA/BF, (D)40% n-HA/BF.

XRD investigation

To further understand the phase structure of n-HA/BF membrane, XRD pattern is given in Fig.3. Obviously, the amorphous peak at 20.5° was the peak of bamboo fiber (Guimaraes et al., 2015), marked with “♦”, and the peaks at 25° and 31° of n-HA were found, noted as “♣” (Ma et al., 2020). The crystallization peak position of n-HA in the composite membrane did not change, indicating that the two components of n-HA and BF were only blended. Similarly, the crystallization peaks of n-HA in Fig.3 (f), (g), (h) were also obviously weaker than those in Fig.3 (c), (d) and (e). This was because the content of n-HA in the membrane formed in oven was less than that in the membrane formed in air, which led to weaker crystal peak in the spectrum. With the increase of n-HA content, the characteristic peak and its crystallinity of n-HA in different membrane increased, which also confirmed that n-HA and BF were only blended without chemical reaction.

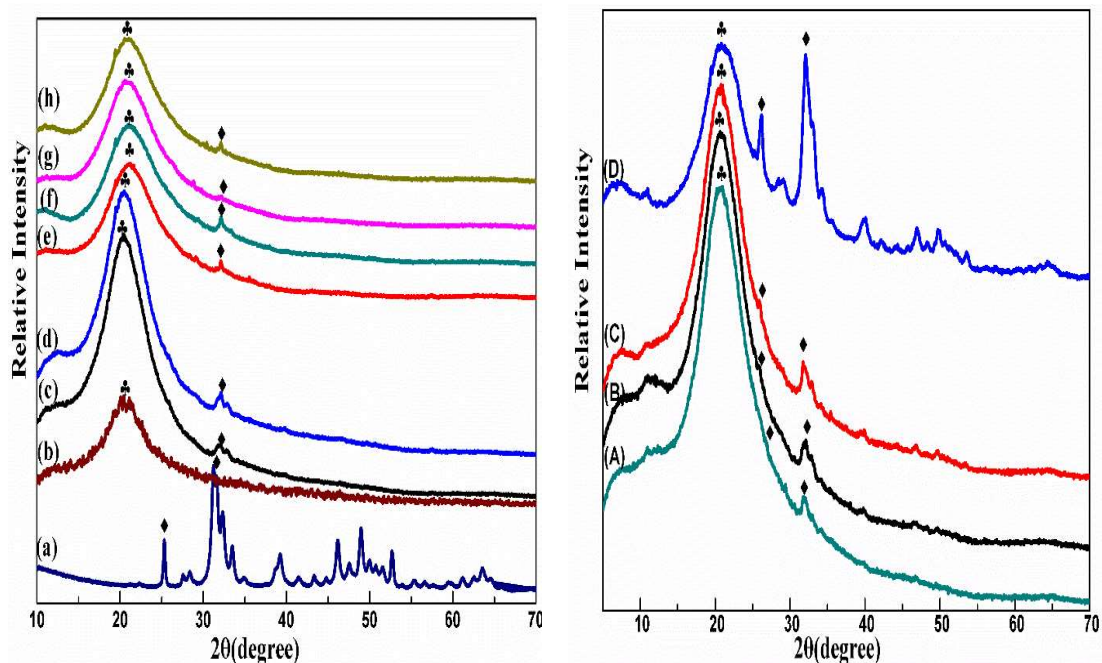


Fig. 3 XRD of samples. (a) n-HA, (b)BF, (c) Air-Air, (d) Air-oven, (e) Air-freeze drying, (f) Oven-air, (g) Oven-oven, (h) Oven-freeze drying, (A) 10% n-HA/BF, (B) 20% n-HA/BF, (C) 30% n-HA/BF, (D) 40% n-HA/BF.

SEM observation

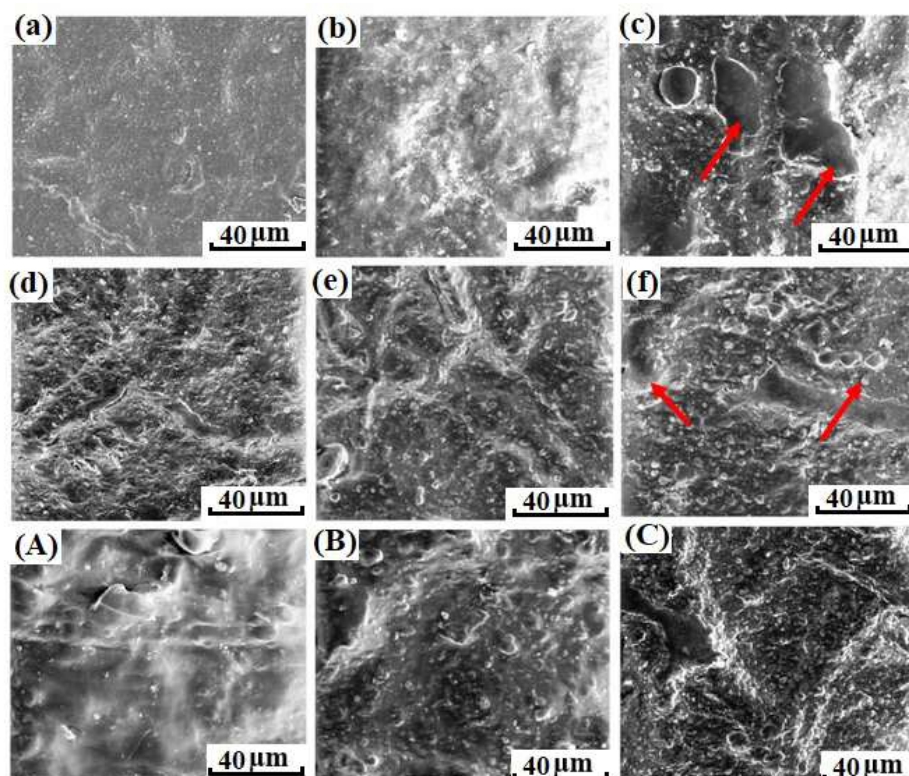


Fig. 4 SEM of samples. (a)Air-Air, (b)Air-oven, (c)Air-freeze drying, (d)Oven-air, (e)Oven-oven, (f)Oven-freeze drying, (A)10%HA/BF, (B) 30%HA/BF, (C)40%HA/BF.

Fig. 4 shows the morphologies of n-HA/BF composite membranes achieved by different methods. According to SEM micrographs, it can be seen that white particles existed in the composite membranes, which proved the existence of n-HA. However, there was subtle difference for the dispersion of n-HA particles in the membrane, and the n-HA was relatively more uniform in oven (Fig.4(d), (e), (f)) than in air (Fig.4(a), (b), (c)), which was caused by the different changes of hydrogen bond between molecules during the forming membrane of bamboo fiber. In oven, the solvent of DMAC was evaporated at high temperature, and the fiber morphology had been fixed before the hydrogen bond shrinking between bamboo fiber molecules, which would bring out better dispersion of n-HA. However, for the three different dry methods, the surfaces were compact without porous structures, and there was no obvious difference for the surface in air and in oven, which indicated that drying method in air or in oven

245 had little effect on the membrane morphology after bamboo fiber molding, and the compact
246 structure could effectively prevent the invasion of connective tissue. While for the freeze-drying
247 method, there was some closed pores on the surface of freeze-dried membrane (Fig.4(c), (f)),
248 which was originated from the pores left by the sublimation of water molecules, and the porous
249 structure was conducive for cell adhesion for guided bone regeneration. Additionally, for the
250 composite membranes with different n-HA contents, the white particles gradually increased on
251 the surface of the membrane, but there was no obvious agglomeration phenomenon, and there
252 was no cavity between n-HA and BF, which indicated that the n-HA/BF composite membrane
253 had good compositional compatibility of hydrophilic n-HA and BF.

254 Contact angle measurement

255 To further make clear the hydrophilicity of the n-HA/BF composite membrane, the contact
256 angle of the n-HA/BF composite membranes were tested with rotating drop interfacial
257 tensiometer by dropping distilled water onto the liquid surface, and the results are shown in
258 Fig.5. As expected, the contact angle of all n-HA/BF casting membranes were less than 90 °,
259 which proved that n-HA/BF casting membranes were hydrophilic membrane. Comparing with
260 the membranes obtained by different methods, it could be found that the same forming
261 membrane method had little effect on the contact angle (Fig.5(a) \approx 5(b), 5(d) \approx 5(e)), while the
262 freeze-dried membrane possessed lower contact angle because of the rough membrane surface
263 with the porous structure (Fig.5(c) and 5(f)), and the stronger hydrophilicity would be more
264 useful for cell adhesion and proliferation (Dhinasekaran et al., 2021). However, for the same
265 dried method, the membrane formed in oven had lower contact angle than that of the membrane
266 formed in air (Fig.5(d) < Fig.5(a), Fig.5(e) < Fig.5(b)), and the reason was that the hydrogen

bonds between the bamboo fibers molecules was destroyed and the surface tension was reduced when the membrane was formed in oven. In addition, for the n-HA/BF composite membranes with different n-HA contents, the contact angle gradually decreased with the increasing of n-HA, which suggested that the higher n-HA content brought about better hydrophilicity of the membrane.

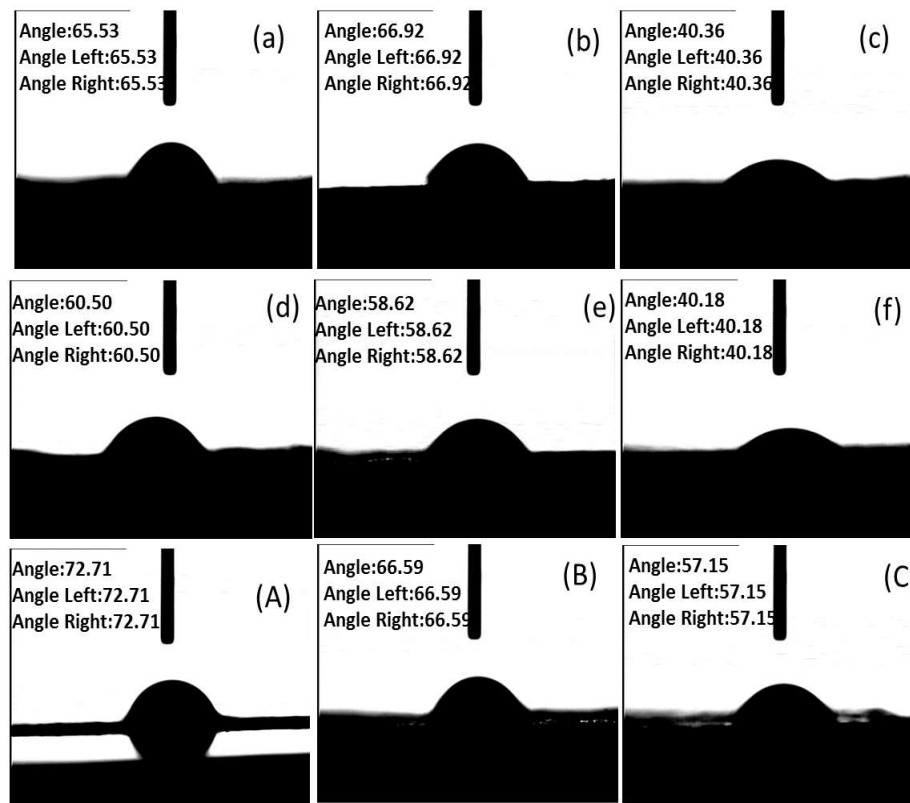


Fig.5. Contact angle of the n-HA/BF composite membranes obtained by different methods. (a) Air-Air, (b) Air-oven, (c) Air-freeze drying, (d) Oven-air, (e) Oven-oven, (f) Oven-freeze drying, (A) 10%-n-HA/BF, (B) 30% n-HA/BF, (C) 40% n-HA/BF.

Tensile strength test

Fig. 6 is the tensile strengths of all the n-HA/BF composite membranes. We found that membrane formed in air had higher mechanical strength than that in oven. Comparing to the membrane formed in air (Fig.6 (a), (b), (c)), the tensile strength of membrane dried by freeze-drying was the worst, and the tensile strength of the membrane dried in air was improved

by 69.64%, and dried in oven was increased by 51.7% than dried by freeze-drying, respectively. Likely, for the three membranes formed in oven (Fig.6(d), (e) and (f)), the tensile strengths of the membranes dried in air and in oven were improved by 23.89% and 5%, respectively. The reason was that the freeze-drying membrane was porous structure, and the forming membrane or dry membrane in oven caused the destruction of intermolecular hydrogen bond during molding, resulting in thinner membrane and larger area, so as to possessed lower tensile strength. For the n-HA/BF composite membranes with different n-HA contents, the tensile strength increased at first but decreased with the increasing of n-HA content, and the 20% n-HA/BF composite membrane represented the highest tensile strength, which was accord with the principle of nanoparticles filler reinforce polymer (Yadav et al., 2020), and the mechanical strength could meet the application requirement of GBR membrane (Castro et al., 2018).

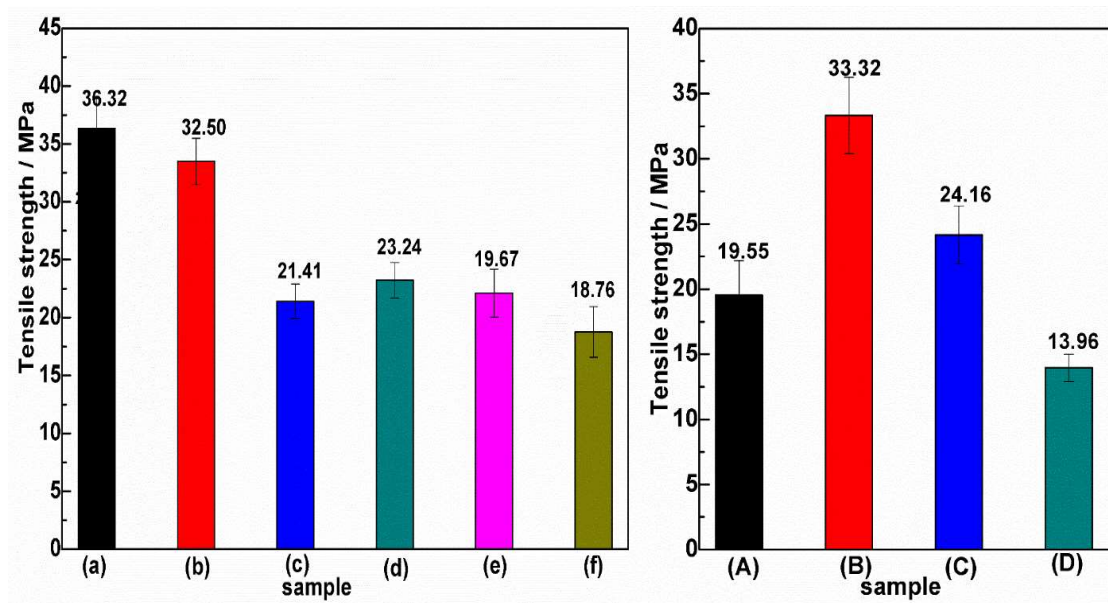


Fig.6. Tensile strength of the samples. (a) Air-Air, (b) Air-oven, (c) Air freeze drying, (d) Oven-air, (e) Oven-oven, (f) Oven-freeze drying, (A) 10% n-HA/BF, (B) 20% n-HA/BF, (C) 30% n-HA/BF, (D) 40% n-HA/BF.

***In vitro* degradation and cell culture**

Weight loss of composite membrane after degradation

Fig.7 gives the weight loss rate of the n-HA/BF composite membranes. It can be seen that the weight loss rate of the composite membrane first decreased and then increased within 8 weeks. During the first 4 weeks, the weight loss rate was negative continuously, which indicated that the mass of composite membrane did not decrease but increased after immersion, meaning that the amount of apatite deposited on the surface of the membrane was greater than the mass of degradation, so that the total mass of composite membrane was greater than that before immersion. Similarly, the weight loss rate of 4-8 weeks was negative, but exhibited an upward trend, suggesting that the membrane had more visible degradation trend. Comparing to the different composite membranes, the weight loss rate of the membrane obtained by oven-freeze drying method changed the most among the membrane different methods, which indicated that bone like apatite adhered the most owing to the porous structure, and the more apatite deposition would have better biological activity. Moreover, for the composite membranes with different n-HA contents, the higher the content of n-HA, the greater the negative value of weight loss rate, which revealed that the higher content of n-HA was more favorable for the bone-like apatite deposition (Kumar et al., 2014).

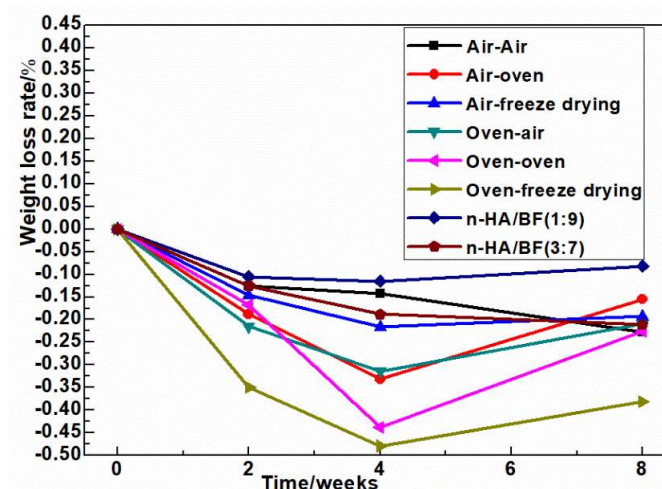


Fig.7 Weight loss rate of samples in SBF.

Water absorption of composite membrane after degradation

Fig.8 is the water absorption of n-HA/BF composite membrane. The results indicated that the water absorption of n-HA/BF composite membrane had a similar trend during the immersion process, that is, the water absorption increased slightly at the initial degradation, and then decreased a little from 4 weeks to 8 weeks, which was caused by the bone-like apatite deposition with the extension of soaking time. Moreover, the freeze-dried membrane had the lowest water absorption, and the main reason was that the porous structure had the fastest degradation, which would produce much micropore and bring more apatite deposition, and it could be proved by the weight loss result. Similarly, for the composite membrane with different n-HA contents, the higher BF content, the higher water absorption had, which was related to the water absorption of BF. In a word, the water absorption results indicated that the n-HA/BF composite membrane had good degradation and water absorption performance.

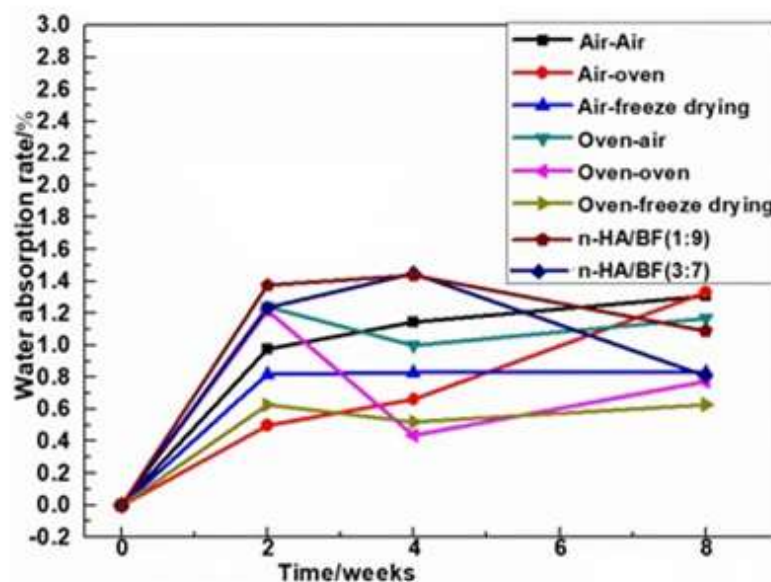


Fig.8. Water absorption rate of samples in SBF.

SEM observation of composite membrane after degradation

Fig. 9 shows the surface morphology of n-HA/BF composite membrane after soaking in SBF for

8 weeks. It can be found that new bone like apatite was **disposited** on the surface of the n-HA/BF composite membrane. However, comparing to the different composite membranes, the composite membrane formed **in air** had less bone like apatite (seen Fig.9 (a), (b), (c)) than the membrane formed **in oven** (seen Fig.9 (d), (e), (f)). The reason was that the hydrogen bond **shrank** between **bamboo fiber molecules**, and n-HA particles were wrapped in the inner part of the membrane when the membrane was formed **in air**. While the composite membrane was formed in the oven, the intermolecular hydrogen bond was broken, and n-HA particles were dispersed on the surface of the membrane, which was more conducive to the deposition of bone-like apatite on the surface of the membrane, and the bone-like apatite would help to improve interface between the tissue-implant and its surrounding tissues (Zhu et al., 2020).

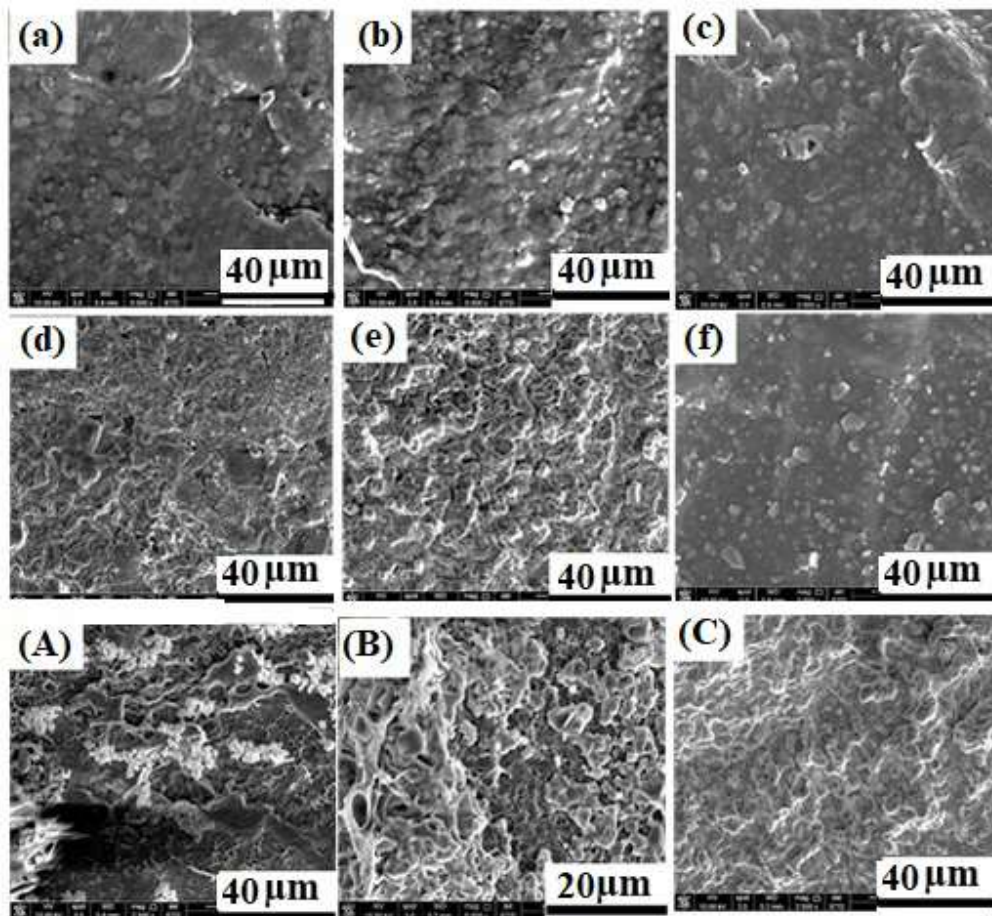


Fig. 9. SEM micrographs of samples after soaking for 8 weeks. (a) Air-Air, (b) Air-oven, (c) Air-freeze drying, (d) Oven-air, (e) Oven-oven, (f) Oven-freeze drying, (A) 10% n-HA/BF, (B) 30% n-HA/BF, (C) 40% n-HA/BF.

For the composite membrane with different n-HA contents of 10%, 30% and 40% n-HA (seen Fig.9(A), (B), (C)), respectively. From the 10% n-HA/BF composite membrane, it can be seen that there were pores on the surface of bamboo fiber (Fig.9(A)), which indicated that bamboo fiber could be degraded during soaking. With the increase of n-HA content, the more bone-like apatite was deposited, which further demonstrated that the n-HA in composite membrane could induce bone-like apatite deposition, and the results were consistent with the previous analysis.

MTT test of cell culture

The cell proliferation results of BMSC cultured on the surface of n-HA/BF composite membrane for 1, 2 and 3 days are given in Fig. 10.

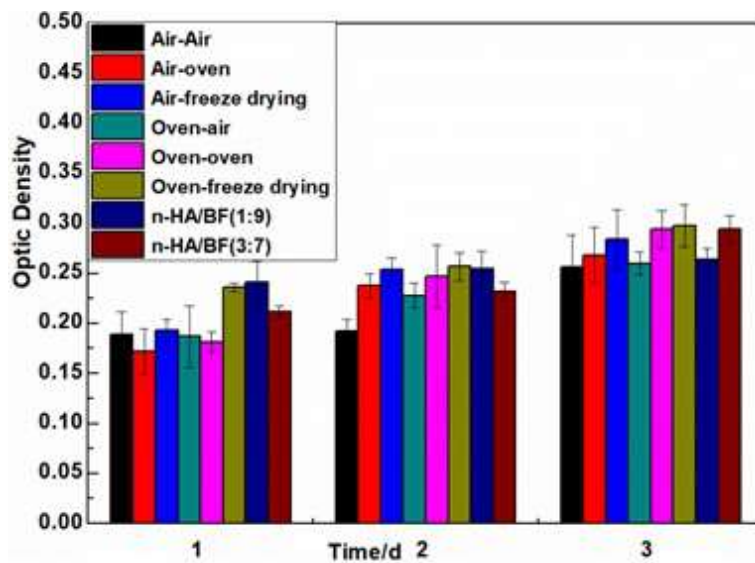


Fig. 10. MTT value of cell culture on sample surface.

It can be seen that the OD value of each sample increased significantly with the extension of culture time, indicating that cells could normally grow and proliferate on different membrane surfaces. In addition, the OD values of freeze-dried composite membrane were significantly higher than those of the membrane dried in air or in oven, which further indicated that the porous

399 structure of freeze-dried composite membrane was more conducive for cell proliferation and
400 possessed better biocompatibility (Ai et al., 2021). Comparing to the n-HA/BF membranes with
401 10%, 20% and 30%, the OD value enhanced significantly with the increase of n-HA content and
402 the extension of culture time. The results illustrated that the cells proliferated rapidly on the
403 surface of the membrane, suggesting that the n-HA/BF composite membrane had good biological
404 properties (Bee et al., 2019). This was consistent with the previous *in vitro* immersion analysis.

405 Conclusions

406 In this study, the n-HA/BF composite membrane was successfully prepared by a simple casting
407 technology, and the effects of different forming membrane, drying methods, and different n-HA
408 contents on the properties of the composite membranes were studied. The results confirmed that
409 there was no chemical bonding between n-HA and BF components, however, the membrane
410 formed in air was thicker than that in oven, because the hydrogen bond shrinkage made the BF
411 gel and DMAC/LiCl solution precipitated from the edge in air. Thus, the tensile strength of the
412 membrane formed in air were higher than that of in oven, especially, the 20 % n-HA/BF
413 composite membrane was the highest, but the tensile strength of freeze-dried composite
414 membrane was the worst because of the porous structure. The contact angle test of the composite
415 membrane confirmed that the composite membrane was hydrophilic, and the freeze-dried
416 membrane exhibited better hydrophilicity owing to the rough surface and the small surface
417 tension. SBF soaking results indicated that n-HA/BF composite membrane displayed different
418 degradability behaviours, and the higher n-HA content in composite membrane possessed better
419 bone-like apatite deposition. The cell proliferation results proved that the composite membranes
420 had no cytotoxicity. This study would provide a new way for developing a novel GBR membrane

421 based on the utilization of natural BF.

422 **Acknowledgement**

423 The authors would like to thank the support of the Natural Science Foundation of Hunan
424 province (2020JJ4430), and Key projects of Hunan Provincial Department of Education
425 (20A315).

426 **References**

- 427 Ai CC, Liu L, Goh JCH (2021). Pore size modulates in vitro osteogenesis of bone marrow mesenchymal stem
428 cells in fibronectin/gelatin coated silk fibroin scaffolds. *Mat Sci Eng. C-Mater.*124: 112088.
- 429 Bee SL, Hamid ZAA (2019). Characterization of chicken bone waste-derived hydroxyapatite and its
430 functionality on chitosan membrane for guided bone regeneration. *Compos Part B-Eng.* 163: 562-573.
- 431 Bierhalz ACK, Moraes AM (2017). Composite membranes of alginate and chitosan reinforced with cotton or
432 linen fibers incorporating epidermal growth factor. *Mat Sci Eng. C-Mater.* 76: 287-294.
- 433 Castro AGB, Diba M, Kersten M, Jansen JA, van den Beucken JJJP, Yang F (2018). Development of a
434 PCL-silica nanoparticles composite membrane for Guided Bone Regeneration. *Mat Sci Eng. C-Mater.* 85:
435 154-161.
- 436 Chesley M, Kennard R, Roozbahani S, Kim SM, Kuk K, Mason M (2020). One-step hydrothermal synthesis
437 with in situ milling of biologically relevant hydroxyapatite. *Mat Sci Eng. C-Mater.* 113: 110962.
- 438 Chingakham C, Manaf O, Sujith A, Sajith V (2020). Hydrophobic nano-bamboo fiber-reinforced acrylonitrile
439 butadiene styrene electrospun membrane for the filtration of crude biodiesel. *Appl Nanosci.* 10: 795-806.
- 440 Cai J, Zhou R, Li TT, He JR, Wang GZ, Wang HB, Xiong HG (2018). Bamboo cellulose-derived cellulose
441 acetate for electrospun nanofibers: synthesis, characterization and kinetics. *Cellulose* 25: 391-398.
- 442 Dhinasekaran D, Vimalraj S, Rajendran AR, Saravannan S, Purushothaman B, Subramaniam B (2021).

443 Bio-inspired multifunctional collagen/electrospun bioactive glass membranes for bone tissue engineering
 444 applications. *Mat Sci Eng. C-Mater.* 126: 111856.

445 Guimaraes M, Botaro VR, Novack KM, Teixeira FG, Tonoli GHD (2015). Starch/PVA-based nanocomposites
 446 reinforced with bamboo nanofibrils. *Ind. Crops Prod.* 70: 72-83.

447 Gurunathan T, Mohanty S, Nayak SK (2015). A review of the recent developments in biocomposites based on
 448 natural fibres and their application perspectives. *Compos Part A-Appl S.* 77: 1-25.

449 Hivechi A, Bahrami SH, Siegel RA, Siehr A, Sahoo A, Milan PB, Joghataei MT, Amoupour M, Simorgh S
 450 (2021). Cellulose nanocrystal effect on crystallization kinetics and biological properties of electrospun
 451 polycaprolactone. *Mat Sci Eng. C-Mater.* 121: 111855.

452 Hoornaert A, d'Arros C, Heymann MF, Layrolle P (2016). Biocompatibility, resorption and biofunctionality of
 453 a new synthetic biodegradable membrane for guided bone regeneration. *Biomed. Mater.* 11: 045012.

454 Hoseini SJ, Darroudi M, Oskuee RK, Gholami L, Zak A (2015). Honey-based synthesis of ZnO nanopowders
 455 and their cytotoxicity effects. *Adv. Powder Technol.* 26: 991-996.

456 Jiang T, Carbone EJ, Lo KWH, Laurencin CT (2015). Electrospinning of polymer nanofibers for tissue
 457 regeneration. *Prog. Polym. Sci.* 46: 1-24.

458 Jiang LY, Li Y, Xiong CD, Su SP (2017). Preparation and characterization of a novel degradable
 459 nano-hydroxyapatite/poly(lactic-co-glycolic) composite reinforced with bamboo fiber. *Mat Sci Eng.*
 460 *C-Mater.* 75: 1014-1018.

461 Jiang LY, Li Y, Ma BL, Ding HJ, Su SP, Xiong CD (2018). Effect of Bamboo Fiber Length on Mechanical
 462 Properties, Crystallization Behavior, and in Vitro Degradation of Bamboo Fiber/Nanohydroxyapatite/Poly
 463 (lactic-co-glycolic) Composite. *Ind. Eng. Chem. Res.* 57: 4585-4591.

464 Jiang LY, Ma BL, Li Y, Ding HJ, Su SP, Xiong CD (2019). Effect of bamboo fiber on the degradation

465 behavior and in vitro cytocompatibility of the nano-hydroxyapatite/poly(lactide-co-glycolide)
 466 (n-HA/PLGA) composite. *Cellulose* 26: 1099-1110.

467 Khalil HPSA, Bhat, IUH, Jawaid M, Zaidon A, Hermawan D, Hadi YS (2012). Bamboo Fibre Reinforced
 468 Biocomposites: A Review. *Mater Design* 42: 353-368.

469 Kumar A, Negi YS, Choudhary V, Bhardwaj NK (2014). Microstructural and mechanical properties of porous
 470 biocomposite scaffolds based on polyvinyl alcohol, nano-hydroxyapatite and cellulose nanocrystals.
 471 *Cellulose* 21: 3409-3426.

472 Lee BS, Lee CC, Lin HP, Shih WA, Hsieh WL, Lai CH, Takeuchi Y, Chen YW (2016). Functional
 473 chitosan membrane with grafted epigallocatechin-3-gallate and lovastatin enhances periodontal
 474 tissue regeneration in dogs. *Carbohydr. Polym.* 151: 790-802.

475 Li BW, Liu YH, Zhou YS, You PY, Wang M, Tang L, Deng Y (2020). Development of a novel extracellular
 476 matrix membrane with an asymmetric structure for guided bone regeneration. *Mater Lett* 274: 127926

477 Li WW, Ma GW, Brazile B, Li N, Dai W, Butler JR, Claude AA, Wertheim JA, Liao J, Wang B (2015).
 478 Investigating the Potential of Amnion-Based Scaffolds as a Barrier Membrane for Guided Bone
 479 Regeneration. *Langmuir* 31: 8642-8653.

480 Li Y, Jiang LY, Xiong CD, Peng WJ (2015). Effect of Different Surface Treatment for Bamboo Fiber on the
 481 Crystallization Behavior and Mechanical Property of Bamboo Fiber/Nanohydroxyapatite/Poly(lactic-co-
 482 glycolic) Composite. *Ind. Eng. Chem. Res.* 54: 12017-12024.

483 Liu D, Song J, Anderson DP, Chang PR, Hua Y (2012). Bamboo Fiber and Its Reinforced Composites:
 484 Structure and Properties. *Cellulose* 19: 1449-1480.

485 Long HB, Wu ZQ, Dong QQ, Shen YT, Zhou WY, Luo Y, Zhang CQ, Dong XM (2019). Effect of
 486 polyethylene glycol on mechanical properties of bamboo fiber-reinforced polylactic acid composites. *J*

487 Appl Polym Sci 136: 47709.

488 Ma BL, Jiang LY, Tang CY, Tang S, Su SP, Shu Y(2020). Preparation and properties of biomimetic
 489 hydroxyapatite-based nanocomposite utilizing bamboo fiber. Cellulose 27: 2069-2083.

490 Ma FB, Xia XY, Tang B (2019). Strontium chondroitin sulfate/silk fibroin blend membrane containing
 491 microporous structure modulates macrophage responses for guided bone regeneration. Carbohyd. Polym
 492 213: 266-275.

493 Mora-Boza A, Garcia-Fernandez L, Barbosa FA, Oliveira AL, Vazquez-Lasa B, San RJ (2020).
 494 Glycerylphosphate crosslinker as a potential osteoinductor of chitosan-based systems
 495 for guided bone regeneration. Carbohyd. Polym. 213: 266-275.

496 Muhammad AN, Emel Y, Iskender Y (2017). Intercalated chitosan/hydroxyapatite nanocomposites: Promising
 497 materials for bone tissue engineering applications. Carbohyd Polym.175: 38-46.

498 Niu XL, Wang LF, Xu MJ, Qin M, Zhao LQ, Wei Y, Hu YC, Lian XJ, Liang ZW, Chen S, Chen WY, Huang
 499 D (2021). Electrospun polyamide-6/chitosan nanofibers reinforced nano-hydroxyapatite/polyamide-6
 500 composite bilayered membranes for guided bone regeneration. Carbohyd. Polym. 260:117769.

501 Oksana Z, Wu XF, Zhou ZP, Ted A, Jivan T, John H (2020). A Comparative Experimental Study of the
 502 Hygroscopic and Mechanical Behaviors of Electrospun Nanofiber Membranes and Solution-cast Films of
 503 Polybenzimidazole. J Appl Polym Sci. 137: e49639.

504 Pappu A, Pickering KL, Thakur VK (2019). Manufacturing and characterization of sustainable hybrid
 505 composites using sisal and hemp fibres as reinforcement of poly (lactic acid) via injection moulding. Ind.
 506 Eng. Chem. Res.137: 260-269.

507 Phuong HAL, Ayob NAI, Blanford CF, Rawi NFM, Szekely G (2019). Nonwoven Membrane Supports from
 508 Renewable Resources: Bamboo Fiber Reinforced Poly (Lactic Acid) Composites. ACS Sustain Chem Eng

509 7: 11885-11893.

510 Priyadarshini B, Vijayalakshmi U (2018). Development of cerium and silicon co-doped hydroxyapatite
 511 nanopowder and its in vitro biological studies for bone regeneration applications. Adv. Powder Technol.
 512 29: 2792-2803.

513 Prajatelista E, Sanandiya ND, Nurrochman A, Marseli F, Choy S, Hwang DS (2021). Biomimetic Janus chitin
 514 nanofiber membrane for potential guided bone regeneration application. Carbohydr. Polym. 251: 117032.

515 Shakeri A, Khakdan F, Soheili V, Sahebkar A, Rassam G, Asili J (2014). Chemical composition, antibacterial
 516 activity, and cytotoxicity of essential oil from *Nepeta ucrainica* L. spp. *Kopetdagensis*. Ind. Crops Prod.
 517 58: 315-321.

518 Tang S, Jiang LY, Ma BL, Tang CY, Wen Y, Zhang N, Zhang Y, Su SP (2020). Preparation and
 519 characterization of bamboo fiber/chitosan/nano-hydroxyapatite composite membrane by ionic crosslinking.
 520 Cellulose 27: 5089-5100.

521 Weng RG, Huang X, Liao DQ, Xu S, Peng L, Liu XZ (2020). A novel cellulose/chitosan composite
 522 nanofiltration membrane prepared with piperazine and trimesoyl chloride by interfacial polymerization.
 523 RSC Adv 10: 1309-1318.

524 Yadav S, Gangwar S (2020). The effectiveness of functionalized nano-hydroxyapatite filler on the physical
 525 and mechanical properties of novel dental restorative composite. Cellulose 69: 907-918.

526 Ye HL, Zhu JJ, Deng D, Jin SE, Li JD, Man Y (2019). Enhanced osteogenesis and angiogenesis by
 527 PCL/chitosan/Sr-doped calcium phosphate electrospun nanocomposite membrane for guided bone. J Biomat
 528 Sci-Polym E 30: 1505-1522.

529 Yu L, Cai Y, Wang H, Pan LB, Li JY, Chen S, Liu Z, Han FX, Li B (2020).
 530 Biomimetic bone regeneration using angle-ply collagen membrane-supported cell sheets subjected to

531 mechanical conditioning. *Acta Biomater* 112: 75-86.

532 Zhao XJ, Zhou LY, Li QD, Zou QX, Du C (2018). Biomimetic mineralization of carboxymethyl chitosan

533 nanofibers with improved osteogenic activity in vitro and in vivo. *Carbohydr Polym.*195: 225-234.

534 Zhu J, Tang D, Lu ZH, Xin ZY, Song J, Meng JM, Lu JR, Li Z, Li JS (2020). Ultrafast bone-like apatite

535 formation on highly porous poly(l-lactic acid)-hydroxyapatite fibres. *Mat Sci Eng. C-Mater.* 116, 11168.

536 Zuo YF, Li WH, Li P, Liu WJ, Li XG, Wu YQ (2018). Preparation and characterization of polylactic

537 acid-g-bamboo fiber based on in-situ solid phase polymerization. *Ind. Crops Prod.* 123: 646-653.

538

539

540

541

542

543

544

545

546

547

548

549

550

551

552

553

554

555

556

557

558

559

560

561

562

563

564

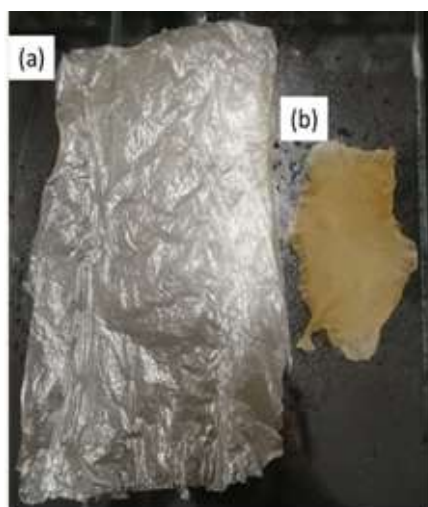
565

566

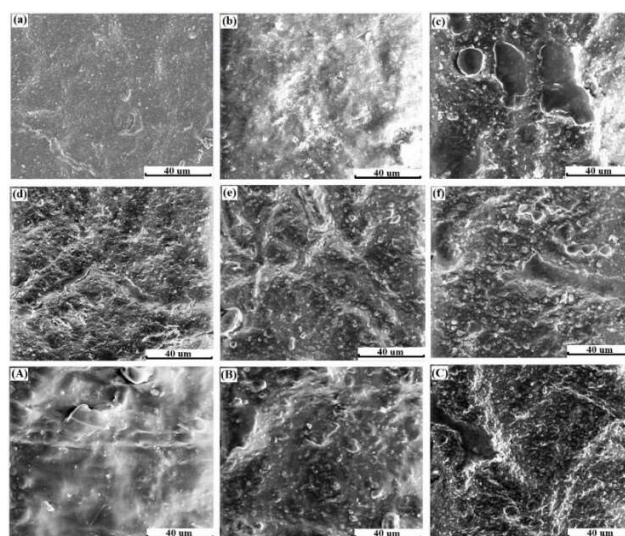
567

Graphical Abstract

In this manuscript, nano-hydroxyapatite/BF (n-HA/BF) composite membrane was prepared by casting method. and the membrane forming mechanism and the effects of different forming membrane methods, drying methods and n-HA amounts on the corresponding n-HA/BF membrane were investigated. Results demonstrated that the morphologies of membrane was determined by the different preparation conditions owing to different hydrogen bond shrinkage. Moreover, the hydrophilicity, the mechanical properties, the degradability and bone-like apatite deposition could be controlled by different preparation conditions, and all the n-HA/BF composite membranes were all non-toxic. The above results indicated that the n-HA/BF composite membrane have a great promising as guide bone tissue regeneration (GBR) membrane, which would provide a new application for BF in biomedical field.



Membrane appearances formed by different conditions. (a) in oven, (b) in air.



SEM micrographs of samples. (a)Air-Air, (b)Air-oven, (c)Air-freeze drying, (d)Oven-air, (e)Oven-oven, (f)Oven-freeze drying, (A)10%HA/BF, (B) 30%HA/BF, (C)40%HA/BF.